

## Research Article

# Preparation and Characterization of Barite/TiO<sub>2</sub> Composite Particles

Hong Zhou, Mengmeng Wang, Hao Ding, and Gaoxiang Du

School of Materials Science and Engineering, China University of Geosciences, Beijing 100083, China

Correspondence should be addressed to Hao Ding; dinghao@cugb.edu.cn

Received 26 July 2014; Revised 19 September 2014; Accepted 7 October 2014

Academic Editor: Hanlie Hong

Copyright © 2015 Hong Zhou et al. This is an open access article distributed under the Creative Commons Attribution License, which permits unrestricted use, distribution, and reproduction in any medium, provided the original work is properly cited.

To make full use of barite mineral and obtain a kind of composite particles material which has the property of both barite and TiO<sub>2</sub>, the composite particles material with TiO<sub>2</sub> coated on the surface of barite particle was prepared by the method of TiOSO<sub>4</sub> solution chemical hydrolysis and precipitation to form hydrolysis composite, removing the impurities of hydrolysis composite, drying, and calcination in this study. The results were evaluated by the covering power of composites. Composite structure and properties were characterized by means of XRD, SEM, FTIR, and XPS. The results showed that the surface of barite had been coated with rutile TiO<sub>2</sub> uniformly and compactly and the hiding power value and oil absorption value of the composite powder were 18.50 g/m<sup>2</sup> and 15.5 g/100 g, respectively, which had similar pigment performances to TiO<sub>2</sub>. The results also showed that it was mainly the strong chemical bond between barite and TiO<sub>2</sub> that combined them firmly in barite/TiO<sub>2</sub> composite particle (B/TCP).

## 1. Introduction

The resource consumption, environmental pollution, cost ascension, and strong demand problems brought about during the production and application of TiO<sub>2</sub> limit its development seriously. To alleviate these problems and reduce the actual dosage of titanium dioxide, preparing white mineral/TiO<sub>2</sub> composite particle materials with similar pigment properties to TiO<sub>2</sub> caused a widespread concern. Many studies show that mineral surface-coated TiO<sub>2</sub> composite particles can be prepared by adding white mineral, such as kaolinite [1–4], wollastonite [5, 6], montmorillonite [7], sericite [8–10], tourmaline [11], and talc [12, 13] to the titanium salt solution [14]. To make titanium salt solution hydrolyzate (hydrated titanium dioxide, TiO<sub>2</sub>·H<sub>2</sub>O) crystallize, the production needs to be calcined at about 600°C to 900°C. The studies above mainly researched the photocatalytic properties, pigment performance, and UV shielding performance of nanotitanium dioxide. As a result of the selected minerals which were more different from titanium dioxide in density, the prepared composites were easy to layer when mixed with other components and could not be used effectively.

Barite with the main component of BaSO<sub>4</sub> and similar density to titanium dioxide is a significant white nonmetallic mineral. Its high reservation, chemical stability, and low cost in China make it extensively applied in chemical raw materials, drilling mud raw materials, glass raw material, chemical fillers, and so on [15]. This is barite as mineral-TiO<sub>2</sub> composite particles substrate provides the basis. The density of barite was close to TiO<sub>2</sub>, and both were 4.3 and 4.4 g/cm<sup>3</sup>, and the oil absorption is low; therefore, preparing barite/TiO<sub>2</sub> composite powder paint is expected to obtain good effect.

There have been studies in preparing functional composite particles by coating metal oxide on surface of barite particles. Yang et al. [16] prepared Sb-SnO<sub>2</sub>/BaSO<sub>4</sub> conductive powder by chemical precipitation method. Zhou [17] prepared barite loaded with nano-TiO<sub>2</sub> composites using TiOSO<sub>4</sub> and TiCl<sub>4</sub> as titanium source in process of methyl orange degradation. Wang et al. [18] prepared barite/TiO<sub>2</sub> composite particles by coating anatase TiO<sub>2</sub> on the surfaces of barite particles through mechanochemical method. These results showed that the prepared composite powders had certain kind of pigment performance and it was mainly the strong electrostatic attraction between barite and TiO<sub>2</sub> that combined them firmly and then formed B/TCP. Therefore,

the composites' pigment performance and the combination extent between barite and  $\text{TiO}_2$  need to be improved.

To prepare barite coated with  $\text{TiO}_2$  composite particles and combine them firmly, chemical precipitation method was used and the technology was studied in this paper. The preparation process conditions, pigment properties of composites, the structure of B/TCP, and the interaction mechanism between  $\text{TiO}_2$  and barite particles were also investigated in this paper.

## 2. Experimental

**2.1. Raw Materials and Reagents.** The barite (particle size of less than  $10\ \mu\text{m}$ ) used was provided by Antai Minerals Co., Ltd, Hebei Province, China.  $\text{TiOSO}_4$  solution (concentration of  $152\ \text{g}/1000\ \text{mL}$ ) was produced by Jiaozuo Chemical Plant, Henan Province, China. Concentrated sulfuric acid and sodium hydroxide (analytical grade) were both purchased from Jingwen Huabo Commerce Center, Beijing, China.

**2.2. Chemical Precipitation Coating Process.** The process of preparing B/TCP by chemical precipitation method could be expressed as follows:

Barite

Ultra-fine grinding  
Preparation of core material  $\rightarrow$  Fine barite powder

Hydrolysis precipitation of titanyl sulfate  
Preparation of shell material  $\rightarrow$

Barite/Titanium dioxide hydrate

Calcined of hydrolyzate  $\rightarrow$  B/TCP.

(1)

Firstly, a certain amount of barite, grinding media, and distilled water were put into a stirred mill (Type GSDM-003, 3L, Beijing Gosdel Powder & Technology Co., Ltd.) and stirred at a speed of  $1000\ \text{r}\cdot\text{min}^{-1}$ . The ratio of the grinding media to powder fed and the concentration of barite slurry were 4:1 and 45%, respectively. The particle size under different grinding time was measured by BT-1500 type centrifugal sedimentation particle size analyzer. Then the effects of grinding time on performance of B/TCP were studied.

Secondly, the barite powders after grinding for a certain time and distilled water were put into 800 mL of flask and stirred at a certain temperature. Then  $\text{TiOSO}_4$  solution was added in five times. The pH value of the reaction solution was adjusted to 2.5 by adding  $\text{H}_2\text{SO}_4$  and  $\text{NaOH}$  aqueous solution. When the reaction time was reached, the stir was stopped. The precipitate was washed with  $70^\circ\text{C}$  distilled water until it was neutral. After that the washed precipitate was filtrated and then dried.

Finally, the dried samples were calcined in muffle furnace at  $800^\circ\text{C}$  for 1 h. The as-prepared B/TCP samples were kept in a desiccator for characterization.

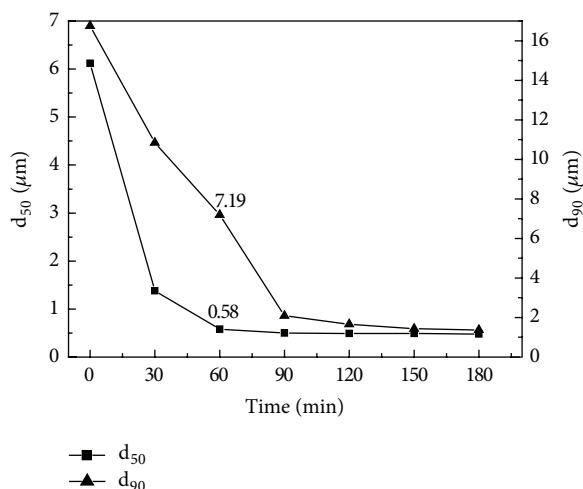


FIGURE 1: Effect of grinding time on granularity about  $d_{50}$  and  $d_{90}$  of barite.

**2.3. Performance and Structure Research Means.** The pigment properties of B/TCP were evaluated and the preparation conditions were optimized by measuring hiding power and oil absorption comprehensively. The hiding power (the minimum mass of pigment used to cover evenly a unit area of background surface when just hiding up its color,  $\text{g}\cdot\text{m}^{-2}$ ) and oil absorption value were measured according to the National Standards GB1709-79 and GB1712-79, respectively.

D/MAX 2000 X-ray powder diffractometer (XRD), made in Rigaku Company, was used to analyze the crystalline phase of B/TCP, and field emission scanning electron microscope, model JSM-7001F, made in Japanese Electronics Company, was used to observe the morphology of raw materials and composite particles. The infrared spectra of powder and the combined form between barite and titanium dioxide were measured by NICOLET 750 type infrared spectroscopy and ESCALAB 250 Xi type X-ray photoelectron spectroscopy spectrometer (XPS), respectively.

## 3. Results and Discussion

**3.1. The Pigment Properties and Structure of B/TCP.** The appropriate proportion between barite and  $\text{TiO}_2$  was the premise of coating  $\text{TiO}_2$  on barite effectively. Hydrolysis complex with barite under different grinding time was prepared. The preparation conditions were as follows: titanyl sulfate solution dosage:  $\text{TiO}_2$  (included in  $\text{TiOSO}_4$  solution): barite = 1:1 (by mass), hydrolysis temperature  $90^\circ\text{C}$ , hydrolysis time 90 min, matrix slurry concentration of barite 1.0%, and the pH value about 2.5. Then B/TCP was prepared after hydrolysis complex was calcined at  $800^\circ\text{C}$  for 1 h. The effects of grinding time and granularity of barite on pigment properties of B/TCP were evaluated by hiding power value and oil absorption value comprehensively. The effects of grinding time on granularity of barite and pigment properties of B/TCP were shown in Figures 1 and 2, respectively.

Figure 1 showed that the granularity about  $d_{50}$  and  $d_{90}$  of barite decreased gradually with grinding time increasing,

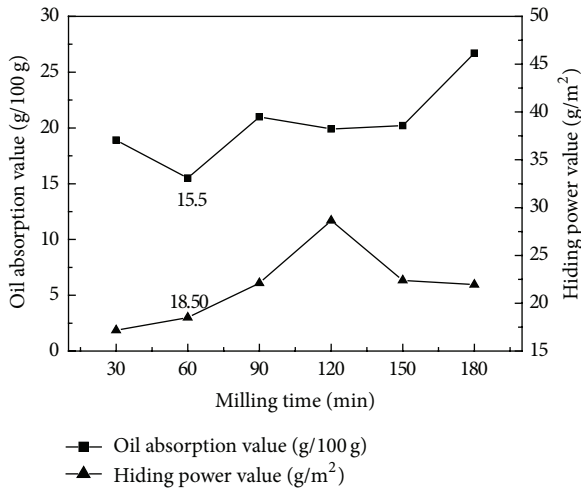


FIGURE 2: Effect of grinding time of barite on pigment properties of B/TCP.

indicating that the particle size was gradually refining. The granularity stabilized to a fixed value 90 min later, indicating that it might turn into a stable state. As shown in Figure 2, the hiding power value of B/TCP prepared first gradually increased and then declined, while the oil absorption value showed an upward trend. When the grinding time of barite reached 60 min, both of the hiding power value and oil absorption value of B/TCP prepared stabilized to a low value, showing that the pigment property was optimal. The granularity about  $d_{50}$  and  $d_{90}$  of barite prepared was  $0.58 \mu\text{m}$  and  $7.19 \mu\text{m}$ , respectively. The hiding power and oil absorption value of B/TCP prepared under optimal conditions were  $18.50 \text{ g/m}^2$  and  $15.5 \text{ g/100 g}$ , respectively. The pigment property of B/TCP prepared was better than the results of B/TCP prepared through mechanochemical method by Wang et al. [18].

Figure 3 showed the SEM images of naked barite and B/TCP prepared with barite under different times.

**3.2. Grinding Time.** It was shown that the naked barite particle had regular square state and smooth surface without tiny covering, while the composite particle with regular state was covered with tiny covering in different degree. It could be deduced that composite particle was composed of barite particle as matrix and the tiny covering was  $\text{TiO}_2$ . Compared with the samples, it could be found that, after barite grinding for 30 min, 60 min, and 90 min, the composite particle had more  $\text{TiO}_2$  which was uniformly and compactly covering its surface, in which after 60 min of grinding and  $\text{TiO}_2$  coating, the composite particles had best covering effect. The result here corresponded to that of Figure 2, which also showed the relevance between structure and properties of B/TCP.

When barite grinding time continued to 120 min and 150 min, there was much area with barite naked on the surface of B/TCP, so  $\text{TiO}_2$  covering degree was lower with worse covering effect. Apparently, the barite grinding time should not be too long during the preparation of B/TCP.

TABLE 1: EDS energy spectrum of naked barite and B/TCP.

Element	Weight percent	Atom percent
O	26.40	63.19
Mg	2.84	4.47
S	12.26	14.65
Ca	2.03	1.94
Ba	56.47	15.75
Total quality	<b>100.00</b>	
C	4.68	12.84
O	28.67	59.03
S	7.32	7.52
Ti	14.23	9.79
Ba	45.10	10.82
Total quality	<b>100.00</b>	

**3.3. X-Ray Diffraction Analysis.** The XRD patterns of naked barite, rutile and anatase  $\text{TiO}_2$ , and B/TCP prepared from barite- $\text{TiOSO}_4$  hydrolysis complex after calcination at different temperature were shown in Figure 4. It showed that the XRD peaks appearing at  $2\theta = 25.8, 26.8, 28.8, 31.5,$  and  $43.0$  were ascribed to that of barite; the XRD peaks appearing at  $2\theta = 27.4, 36.8, 42.6, 54.3,$  and  $56.6^\circ$  were ascribed to that of rutile  $\text{TiO}_2$ ; the XRD peaks appearing at  $2\theta = 25.3, 37.8, 48.1,$  and  $55.1^\circ$  were ascribed to that of anatase  $\text{TiO}_2$ . Otherwise, little anatase  $\text{TiO}_2$  diffraction peaks were generated when hydrolysis complex was calcined at less than  $700^\circ\text{C}$ , without rutile  $\text{TiO}_2$  characteristic peak. It could be deduced that there was little  $\text{TiOSO}_4$  hydrolysate on the surface of barite transformed into anatase crystalline phase. Almost all of  $\text{TiO}_2$  on the surface of composite changed into rutile  $\text{TiO}_2$  when calcined temperature increased to  $750^\circ\text{C}$  and  $800^\circ\text{C}$  and the diffraction peaks were strong. Meanwhile, the reflections of barite substrate decreased greatly, indicating that composite particle surface had mainly consisted of rutile  $\text{TiO}_2$  and the barite surface was basically covered with  $\text{TiO}_2$ .

**3.4. Scanning Electron Microscope and EDS Energy Spectrum Analysis.** The SEM images of naked barite and B/TCP were shown in Figure 5, and the corresponding EDS spectrum analysis results were shown in Table 1.

Figure 5 showed that barite raw material was composed of regular square particles with smooth surface. It corresponded to the characteristic of orthogonal (oblique) crystal which existed in the form of thick plate-like, columnar, or granular aggregate. While B/TCP was composed of small  $\text{TiO}_2$  particles uniformly and densely, it could be deduced that B/TCP was composed of  $\text{TiO}_2$  coated with barite and  $\text{TiO}_2$  was not aggregate. Obviously, barite was like a crystal core for the generated  $\text{TiO}_2 \cdot \text{H}_2\text{O}$  growing and attached uniformly. And then the Barite- $\text{TiO}_2 \cdot \text{H}_2\text{O}$  composite particles were washed, stirred, filtered, and calcined at high temperature many times during the preparing process. But most of  $\text{TiO}_2$  coating on the surface of barite did not drop off and had regular shape, compact arrangement, and fixed crystal type, indicating that  $\text{TiO}_2$  and barite particle were combined firmly, which corresponded to XRD results.

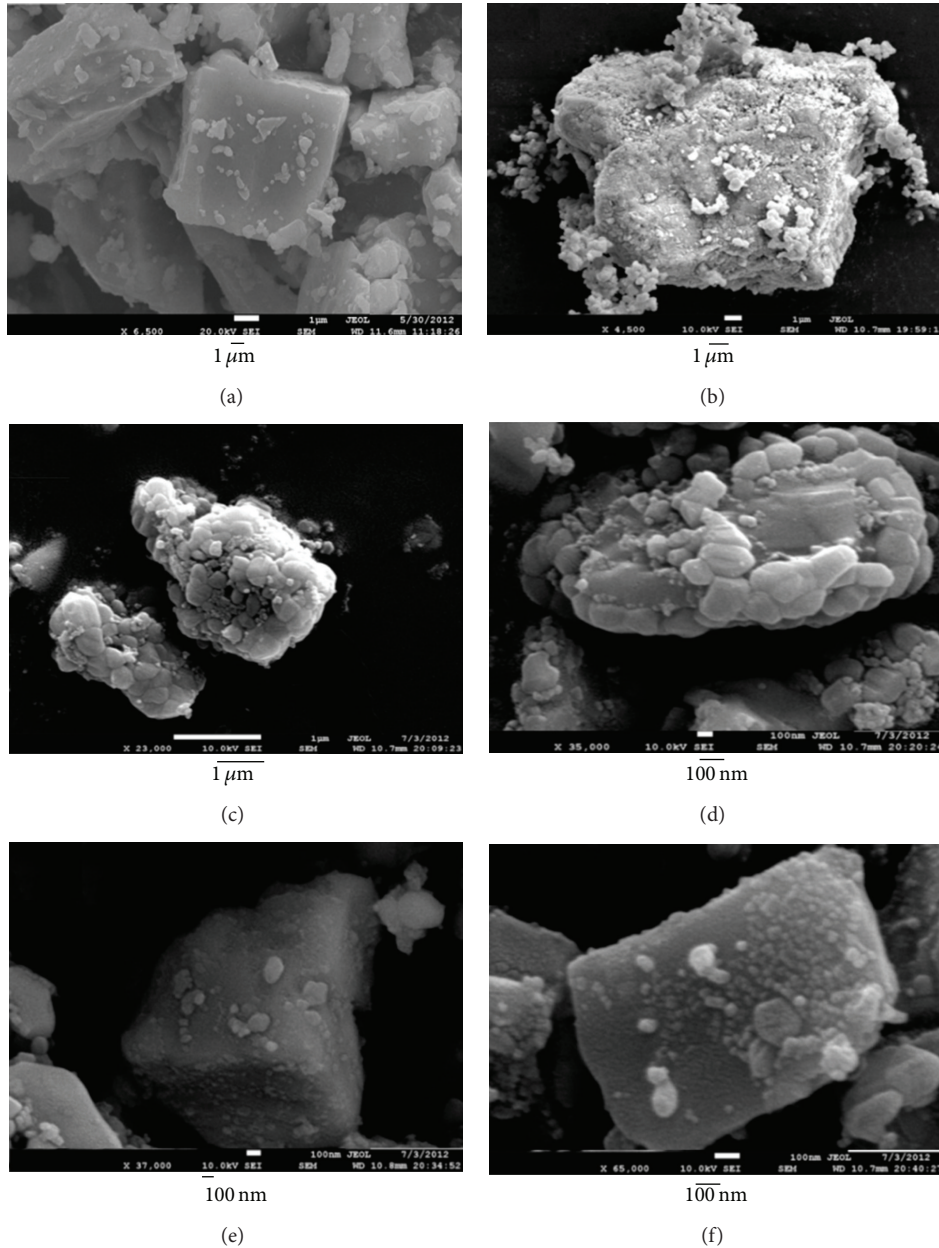


FIGURE 3: SEM images of naked barite (a), 30 min of grinding (b), 60 min of grinding (c), 90 min of grinding (d), 120 min of grinding (e), and 150 min of grinding (f).

As shown in Table 1, the EDS data of barite raw material was consistent with its elements, just a little Ca and Mg, indicating that it was pure. By comparing the EDS spectrum analysis of B/TCP and barite raw material, it could be found that the weight percent of S and Ba significantly decreased, while Ti increased obviously (the weight percent of 14.23%). It was deduced that quantity of  $\text{TiO}_2$  was generated on surface of composites, which corresponded to XRD and the SEM results.

**3.5. IR Spectrum Analysis.** IR spectrograms of rutile  $\text{TiO}_2$ , B/TCP (prepared by calcining at  $800^\circ\text{C}$  for 1h), and barite

were shown in Figure 6. In the spectrogram of rutile  $\text{TiO}_2$ , the IR absorption bands at  $674\text{ cm}^{-1}$  and  $473\text{ cm}^{-1}$  corresponded to vibration of Ti-O. In the spectrogram of barite, the bands at  $1177\text{ cm}^{-1}$ ,  $1115\text{ cm}^{-1}$ , and  $1076\text{ cm}^{-1}$  were assigned to the asymmetric stretching vibration of S-O, resulting from threefold degeneracy of S-O.  $983\text{ cm}^{-1}$  band was assigned to the symmetric stretching vibration of S-O, while bands at  $635\text{ cm}^{-1}$  and  $612\text{ cm}^{-1}$  corresponded to the bending vibration of S-O, which was also from the threefold degeneracy [19]. Therefore, it could be inferred that the IR spectrogram of this section mainly showed the inner vibration mode of  $\text{SO}_4$  group. By comparing Figure 6 (a, b, and c) curve, it

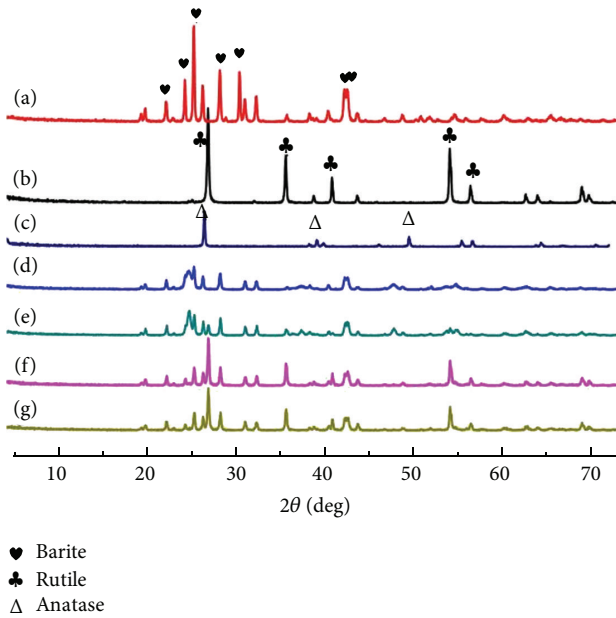


FIGURE 4: XRD patterns of the naked barite (a), rutile  $\text{TiO}_2$  (b), anatase  $\text{TiO}_2$  (c), and barite coated with  $\text{TiO}_2$  powders ((d), (e), (f), and (g)) calcined at 600, 700, 750, and 800°C for 1 h.

was shown that the bands of B/TCP at  $883\text{ cm}^{-1}$ ,  $728\text{ cm}^{-1}$ , and  $1440\text{ cm}^{-1}$  disappeared. Deducing from the above phenomenon, there were some free hydroxyls on the surface of B/TCP before being calcined and then they dropped off after being calcined. It could also be found that the peak at  $612\text{ cm}^{-1}$  in Figure 6(b) turned wider than that in Figure 6(c), deducing that the banding form of  $\text{Ba}^{2+}$  and hydroxyl on the surface of B/TCP might have changed and a new chemical bond  $\text{Ti-O-Ba}$  was formed.

**3.6. XPS Analysis.** As Figures 7, 8, and 9 show, to prove the binding energy of each main characteristic element before and after B/TCP being formed and deduce  $\text{Ti-O-Ba}$  chemical bond formed, the naked barite, rutile  $\text{TiO}_2$ , and B/TCP were characterized with XPS under a  $\text{CuK}\alpha$ -radiation, a power of 150 W, and a background pressure of  $6.5 \times 10^{-10}$  mbar including all elements spectrum diagram and Ba, S, and Ti elements spectrum diagram. The binding energy of  $\text{Ba}_{3d}$  in naked barite was 779.61 eV, while it changed into 780.74 eV in  $\text{TiO}_2$ -coated barite powders. Therefore, the binding energy of  $\text{Ba}_{3d}$  shifted to a higher value about 1.13 eV, indicating that the chemical environment around Ba atom changed. Moreover, the binding energy of  $\text{S}_{2p}$  in raw barite and  $\text{Ti}_{2p}$  in rutile  $\text{TiO}_2$  was 169.00 eV and 458.44 eV, respectively. However, the value changed into 170.02 eV and 458.46 eV, respectively, in B/TCP. Comparing with the binding energy in barite and rutile  $\text{TiO}_2$ , the binding energy of  $\text{S}_{2p}$  and  $\text{Ti}_{2p}$  shifted to a higher value about 1.02 eV and 0.02 eV. From the change above, it could be indicated that the chemical environment around S atom in barite changed apparently after barite covering with  $\text{TiO}_2$ . The binding energy shift of  $\text{Ti}_{2p}$  was lower, deducing that it still combined with O firmly in the form of  $\text{Ti-O}$  bond.

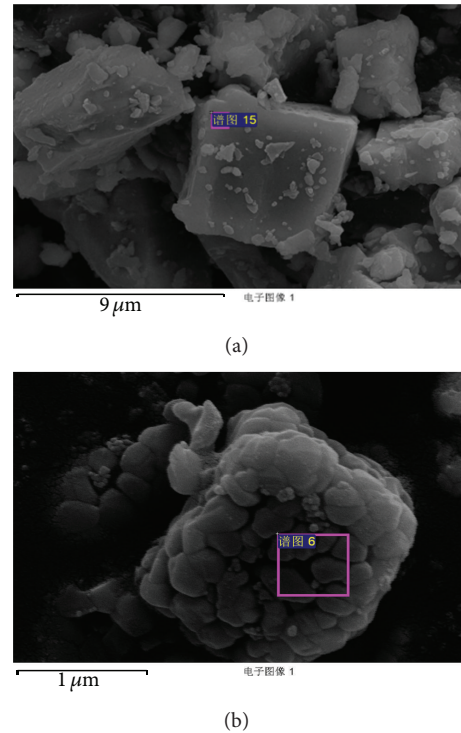


FIGURE 5: SEM images of naked barite (a) and B/TCP (b).

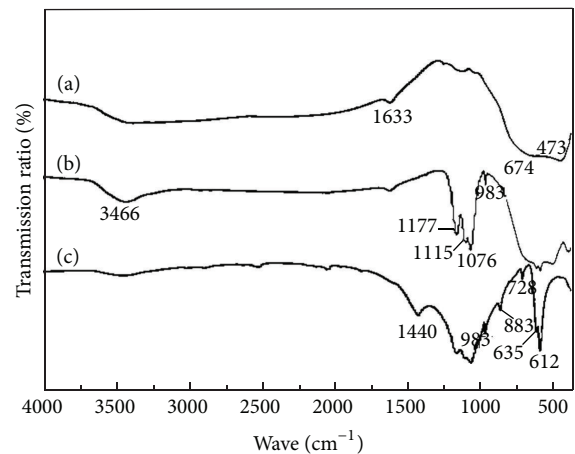


FIGURE 6: IR spectrum of samples: (a) the IR spectrogram of  $\text{TiO}_2$ ; (b) the IR spectrogram of B/TCP; and (c) the IR spectrogram of barite.

As a result of some free hydroxyl groups around Ba atom and Ti atom which exist in  $\text{barite-TiO}_2 \cdot \text{H}_2\text{O}$ , Ba atom and Ti atom were combined by dropping off hydrogen and hydroxyl, forming  $\text{Ti-O-Ba}$  bond. The chemical shift is generated due to the environmental changes of atoms, which is mainly from the potential energy changes caused by valence electron transfer. Valence electron transfer is closely related to the electronegativity of corresponding element [20]. The inner electrons of the atoms are mainly attracted through Coulomb force by nucleus, which makes the electron have a certain binding energy. Meanwhile, the inner electron is

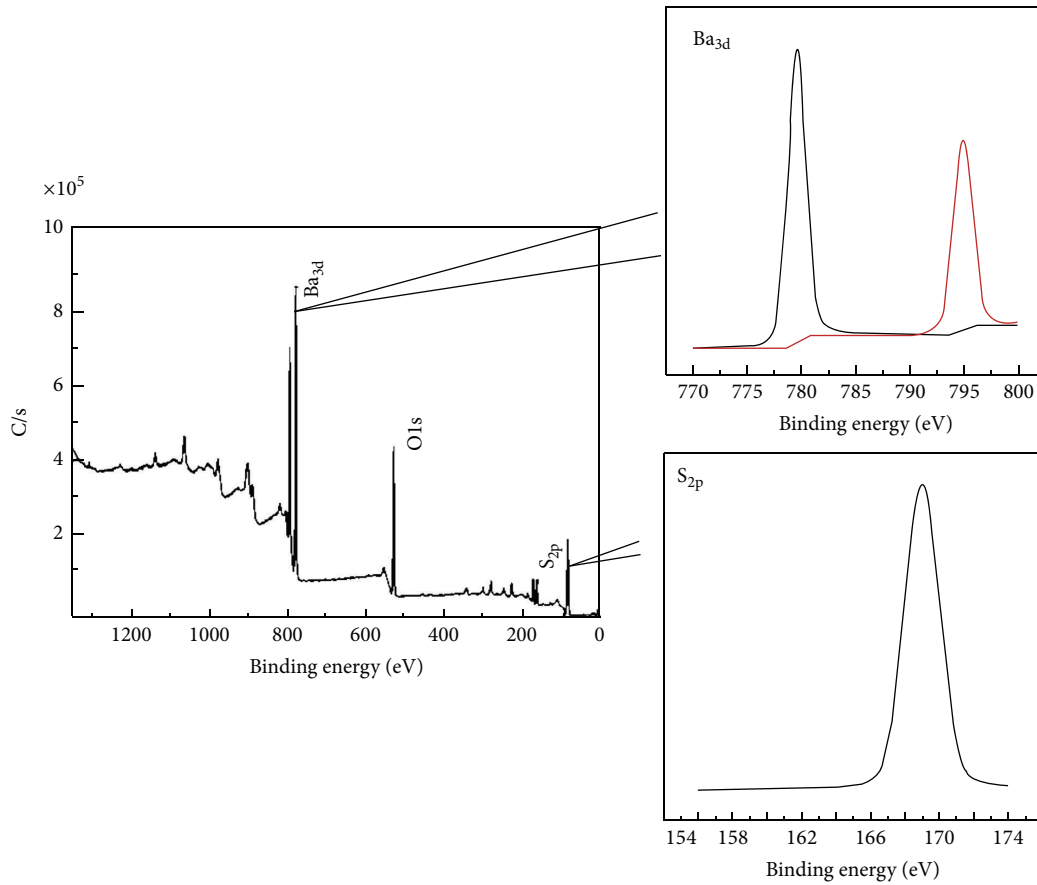


FIGURE 7: XPS spectrum of all elements of barite and XPS spectrum of Ba and S.

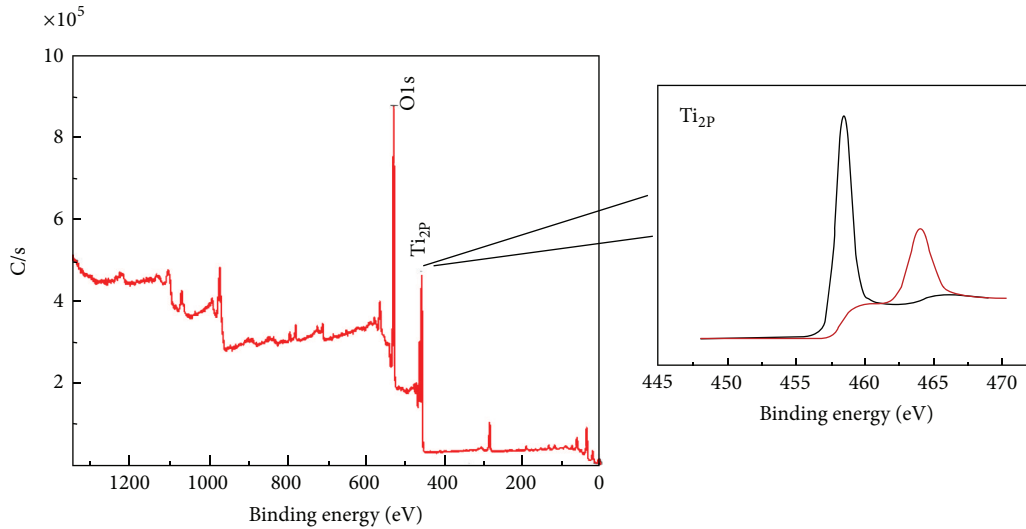


FIGURE 8: XPS spectrum of all elements of rutile TiO<sub>2</sub> and XPS spectrum of Ti.

shielded by the outer electron. Therefore, when the valence electrons shift to the large electronegativity atom, whose electron concentration is increased, the shielding effect is enhanced and the binding energy is decreased. On the contrary, the binding energy will increase. Due to the larger

electronegativity of Ti than that of Ba, the electron around Ba transfers to O-Ti, and then the electron concentration around Ti is increased, the shielding effect is enhanced, and the binding energy is decreased, while the binding energy of Ba is increased.

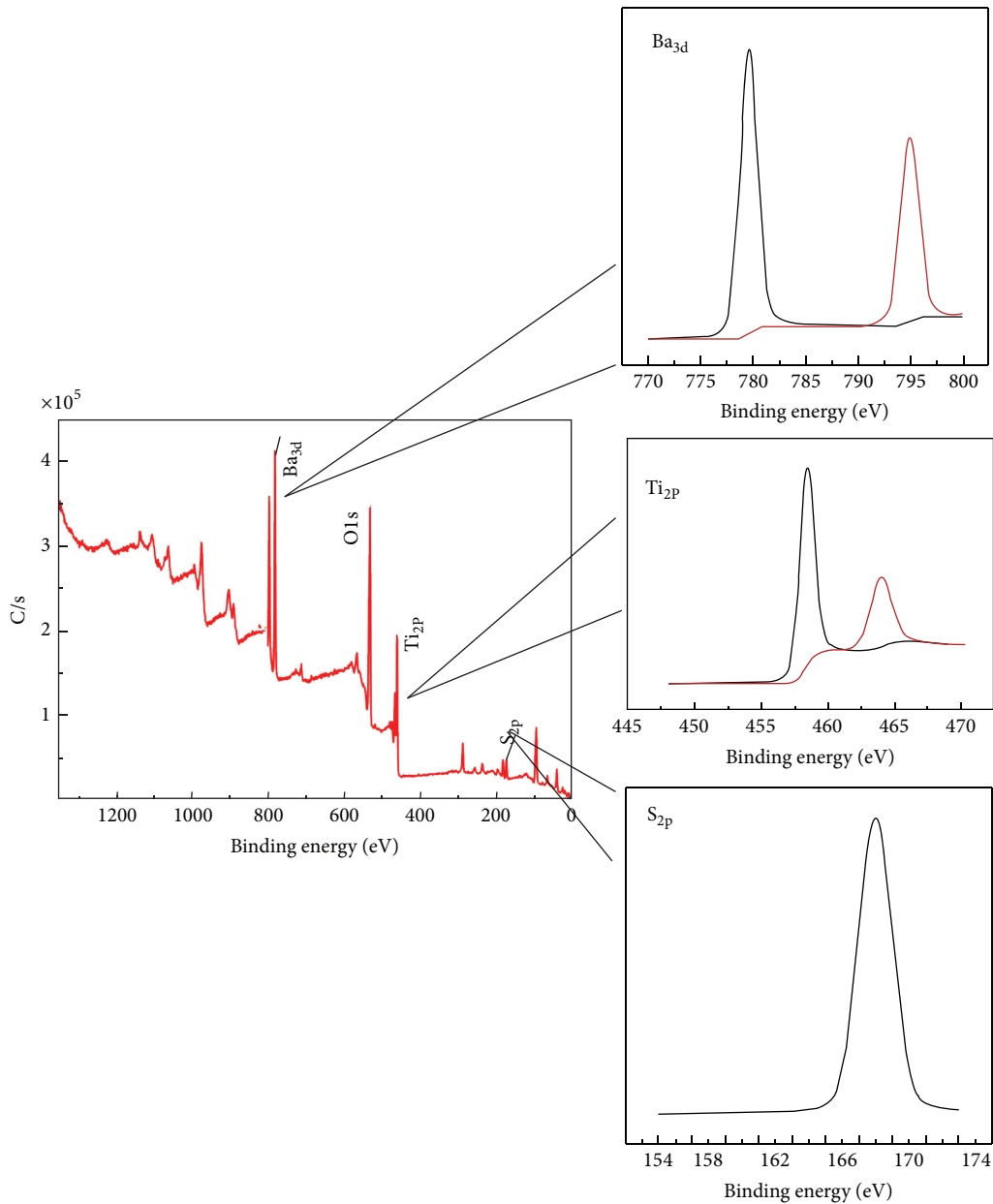


FIGURE 9: XPS spectrum of all elements of B/TCP and XPS spectrum of Ba, S, and Ti.

#### 4. Conclusion

(1) B/TCP was prepared through  $\text{TiOSO}_4$  hydrolysis,  $\text{TiO}_2 \cdot \text{H}_2\text{O}$  depositing and coating on the surfaces of barite, and composite particles calcined method in  $\text{TiOSO}_4$  hydrolysis system including barite. The results showed that the composite powder had similar pigment performances with titanium dioxide and the oil absorption value and hiding power value were 15.5 g/100 g and 18.50 g/m<sup>2</sup>, respectively.

(2) The structure and properties of B/TCP were influenced greatly by the granularity of barite and the calcined temperature of hydrolysis complex. The composite particles with  $\text{TiO}_2$  coating on the surface of barite uniformly and compactly were prepared when the granularity about  $d_{50}$  and

$d_{90}$  of barite was 0.58  $\mu\text{m}$  and 7.19  $\mu\text{m}$ , respectively. When the calcined temperature of hydrolysis complex was over 700 °C, the  $\text{TiO}_2$  on the surface of composite particle was rutile crystalline.

(3) By analyzing the results of IR and XPS, we deduce that barite and  $\text{TiO}_2$  were combined with Ti–O–Ba chemical bond in B/TCP, which made  $\text{TiO}_2$  coat on the surface of barite uniform, compact, and firm.

(4) In the process of preparation of B/TCP, the pigment performance of B/TCP would be more better, when  $\text{TiO}_2$  coated on the surface of barite the more uniformly and compactly, and they combined the more firmly. Therefore, the results show that this study is very useful to improve the pigment performance of B/TCP.

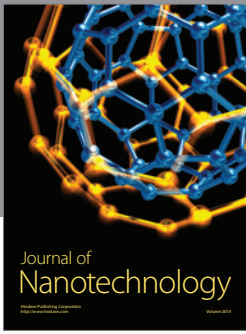
## Conflict of Interests

The authors declare that there is no conflict of interests regarding the publication of this paper.

## References

- [1] Y. Zhang, H. Gan, and G. Zhang, "A novel mixed-phase TiO<sub>2</sub>/kaolinite composites and their photocatalytic activity for degradation of organic contaminants," *Chemical Engineering Journal*, vol. 172, no. 2-3, pp. 936–943, 2011.
- [2] K. Mamulová Kutlákova, J. Tokarský, P. Kovář et al., "Preparation and characterization of photoactive composite kaolinite/TiO<sub>2</sub>," *Journal of Hazardous Materials*, vol. 188, no. 1–3, pp. 212–220, 2011.
- [3] L. Hai, *Research on the Technology and Theory of Preparing Substitute Product of Titanium Dioxide by Use of Calcined Coal Kaolin*, Beijing University of Technology and Science, Beijing, China, 1999.
- [4] L. Hai, "Research on the technology of coating TiO<sub>2</sub> film on the surface of ultra-fine calcined coal kaolin powder," *China Mining Magazine*, vol. 9, pp. 60–64, 2000.
- [5] J.-W. Lee, S. Kong, W.-S. Kim, and J. Kim, "Preparation and characterization of SiO<sub>2</sub>/TiO<sub>2</sub> core-shell particles with controlled shell thickness," *Materials Chemistry and Physics*, vol. 106, no. 1, pp. 39–44, 2007.
- [6] M. Yuan, S. Ren, Y. Guo, X. Zhao, and Y. Liu, "Preparation and characterization of TiO<sub>2</sub>/SiO<sub>2</sub> composites," *Journal of Ji Lin University (Science Edition)*, vol. 45, pp. 857–860, 2007.
- [7] H. Qian, *Research on the Preparation and Degradation Characteristic of Nanometer TiO<sub>2</sub>/Montmorillonite Composite Photocatalytic Materials*, Wuhan University of Technology, Wuhan, China, 2006.
- [8] M. Ren, H. Yin, Z. Lu, A. Wang, L. Yu, and T. Jiang, "Evolution of rutile TiO<sub>2</sub> coating layers on lamellar sericite surface induced by Sn<sup>4+</sup> and the pigmentary properties," *Powder Technology*, vol. 204, no. 2-3, pp. 249–254, 2010.
- [9] M. Ren, H. Yin, A. Wang et al., "Evolution of TiO<sub>2</sub> coating layers on lamellar sericite in the presence of La<sup>3+</sup> and the pigmentary properties," *Applied Surface Science*, vol. 254, no. 22, pp. 7314–7320, 2008.
- [10] R. Jun, *Study on Preparation of Sericite/TiO<sub>2</sub> Composite Particles Material by Hydrolyzing-Coating Method*, China University of Geosciences, Beijing, China, 2008.
- [11] X. Yan, Z. Ji, J. Wang et al., "Preparation and characterization of nano-TiO<sub>2</sub> tourmaline," *Rare Metal Materials and Engineering*, vol. 33, pp. 66–68, 2004.
- [12] N. M. Ahmed and M. M. Selim, "Anticorrosive performance of titanium dioxide-talc hybrid pigments in alkyd paint formulations for protection of steel structures," *Anti-Corrosion Methods and Materials*, vol. 57, no. 3, pp. 133–141, 2010.
- [13] P. Liu, *Preparation and Ultraviolet Shielding Research on Nano-TiO<sub>2</sub>/Talc*, Tianjin University, Tianjin, China, 2005.
- [14] H. Lin and Y. Hu, "Mechanism of coating TiO<sub>2</sub> film on the surface of ultra-fine industrial mineral particles," *The Chinese Journal of Process Engineering*, vol. 2, pp. 151–155, 2002.
- [15] H. Ma, *Industrial Mineral and Rock*, Geological Publishing House, Beijing, China, 2001.
- [16] H. Yang, Y. Hu, H. Zhang, and C. Du, "Preparation and characterization of Sb-SnO<sub>2</sub>/BaSO<sub>4</sub> conductive powder," *Journal of the Chinese Ceramic Society*, vol. 34, no. 7, pp. 776–781, 2006.
- [17] H. Zhou, *Preparation and Photocatalytic Activity of TiO<sub>2</sub>/BaSO<sub>4</sub> Composite Material*, Hebei Normal University, Shijiazhuang, China, 2010.
- [18] B. Wang, H. Ding, Y. Wang et al., "Preparation of Barite/TiO<sub>2</sub> composite particle and interaction mechanism between TiO<sub>2</sub> and Barite particles," *Rare Metal Materials and Engineering*, vol. 40, pp. 193–197, 2011.
- [19] W. Lu, W. Liang, Z. Zhang et al., *Mineral infrared spectroscopy [M.S. thesis]*, Chongqing University Publishing House, Chongqing, China, 1989.
- [20] Y. Lin, T. Wang, and C. Tan, "Organically modified silica-alumina oxide-coated titanium dioxide particles," *Chemical Journal of Chinese Universities*, vol. 22, pp. 104–107, 2001.





**Hindawi**

Submit your manuscripts at  
<http://www.hindawi.com>

